

REDISTRIBUTION OF STRESSES FROM MANUFACTURING OPERATIONS DURING SERVICE LOADS AND THEIR EFFECT ON FATIGUE LIFE OF BUILT-UP STRUCTURES

B Lennart Josefson and Jonas W Ringsberg
Division of Applied Mechanics
Chalmers University of Technology
SE-412 96 Göteborg, Sweden
Lennart.Josefson@me.chalmers.se; Jonas.Ringsberg@me.chalmers.se

Abstract

When manufacturing built-up structures different operations like joining, forming and casting will introduce residual stresses, which will interact with subsequent service loads applied to the structure and also influence growth of cracks in critical locations. This overview addresses the fatigue design of structures considering the effects of residual stresses caused by manufacturing.

The redistribution of residual stresses during operation, the derivation of stress-intensity factors for cracks in residual stress fields and techniques to study growth of cracks in structures containing residual stress fields will be discussed. Joining of components by welding will be discussed in detail. Welding will introduce residual stresses in the structure due to localized plastic deformation caused by strong temperature gradients, with normally, tensile peaks in the welded region where cracks often are initiated due to the stress concentration. The presence of tensile residual, mean, stresses in regions with stress concentrations make welds susceptible to fatigue crack growth, which has led to the development of special design codes for welded joints. The background for such codes and different strategies for the fatigue design will be addressed.

Some recent applications will be discussed in detail, growth of cracks in spot welded car components, in flash butt welded railway rails and in stress coined holes in plates.

Introduction

When built-up structures are manufactured different operations such as joining, forming and casting introduce residual stresses. These stresses interact with additional stresses from subsequent service loads applied to the structure. The history of stresses, distortions and plastic strains may have an important effect of the service life of a structure. Brust [1] illustrates this effect in some examples. The present paper gives an overview of the fatigue design of structures considering the effects of residual stresses caused by manufacturing operations.

Manufacturing processes like joining, grinding or surface treatment introduce residual stresses and distortions in a structure as a consequence of local plastic deformations. In many cases one intentionally introduces compressive stresses on the surface, e.g. hardening and peening. However, in some joining methods like welding the local temperature history consisting of a rapid heating and subsequent cooling phase will generate tensile residual stresses in the welded joint in the location of a medium to high stress concentration.

The presence of residual stresses may be important for the functioning of the structure. Tensile residual stresses will impair the fatigue behaviour of the structure by enhancing the initiation and growth of fatigue cracks, while compressive residual stresses reduce the buckling strength of the structure. It is therefore of interest to estimate the redistribution, and possible relaxation, of residual stresses in a structure subject loaded by design stresses.

The present paper discusses this interaction between residual stresses and stresses caused by design loads, and the assessment of the effect of residual stresses on the growth of fatigue cracks. Due to the large technical interest for the fatigue behaviour of welded joints, we will focus on welds, although some other applications will be discussed.

Residual stresses from manufacturing operations

During welding the material in the joint will be subject to a rapid heating followed by a rapid cooling period. This inhomogeneous temperature field will give local plastic deformations and thus a residual stress field in the structure. The shape and magnitude of the welding residual stress field for different geometries are discussed in Radaj [2]. Lindgren [3-5] and Runesson et al. [6] are recent references where methods for numerical simulation of the welding process thermal, mechanical and microstructure development are discussed. Focus are on material modelling, coupling effects between thermal, mechanical fields and microstructure, numerical techniques and modelling aspects. Dong [7,8] discusses the importance of proper constitutive modelling of the high temperatures behaviour. Stacey et al. [9] presents how residual stresses are accounted for in the SINTAP (Structural Integrity Assessment Procedures for European Industry) defect assessment procedure using analytical methods. The residual stress field is approximated in the analyses using analytical shapes. Common for many weld geometries and welding situations is that this joining method will result in tensile residual stresses in the weld region, often with yield stress magnitude. Further assembling of built-up structures may introduce additional tensile residual stresses due to restrained contraction during cooling after later welding and also due to imperfect fit-up.

Redistribution of residual stresses during service loading

The appearance of local plastic deformations in a structure will lead to the generation of residual stresses. During later and subsequent operational use these stresses will interact with stresses caused by newly applied loads. This will result in a redistribution of the stress field and a new final residual stress field. The residual stress field is important for the function of the structure as it may influence the mechanical behaviour of a structure in several ways. To fully understand the growth of fatigue cracks it is essential to know the stress range acting at the crack. For example, as a result of the development of steel alloys welds are today ductile and not so susceptible to static fracture. However, welds are still susceptible to fatigue failure, which can be explained as follows.

- The joining process will create a geometric discontinuity, which may have a large stress concentration factor (or rather a high fatigue notch factor). This is particularly true for so called fillet welds connecting plates located perpendicular to each other. This means, in practice, that for fillet welds one has already a macroscopic crack after the joining, extending over several grains, present in the weld. Investigations of fillet welds show that cracks with lengths of 0.1 - 0.5 mm will be present. In terms of fatigue one therefore has established a Stage II crack (see Miller [10]).

- The residual stress field will often have a tensile magnitude of yield stress level in the weld (with stress concentration). The resulting stress cycle will have a large mean stress level irrespective of the mean stress level of the applied load. This is because the welding process generates residual stresses at the weld that are assumed (which is also often the case) to reach the yield stress level in tension, which means that the stress at the weld during operation will vary from σ_y to $\sigma_y - \Delta\sigma$, for normal HCF load situations when the applied stress range and maximum stress are considerably lower than the yield stress. This is a worst case scenario which design codes for welded structures are based on. This means that the local R -ratio ($R = \sigma_{\min} / \sigma_{\max}$) is high with tensile stresses acting on the crack-tip during the entire load cycle. The fatigue life is therefore often assumed to be independent of the R -ratio for the external load.

The same load and residual stress situation, with high mean stresses, exists also in pre-stressed bolted or threaded joints. The two factors above will result in only a crack propagation phase with a crack growth rate that may be some 5 - 10 higher than for the case with a geometrical discontinuity without residual stresses. Figure 1 shows the growth in the thickness direction of a surface crack from the toe of a fillet weld in a stiffened plate, with thickness 12.7 mm, subject to an alternating membrane ($R = -1$) stress with different amplitudes.

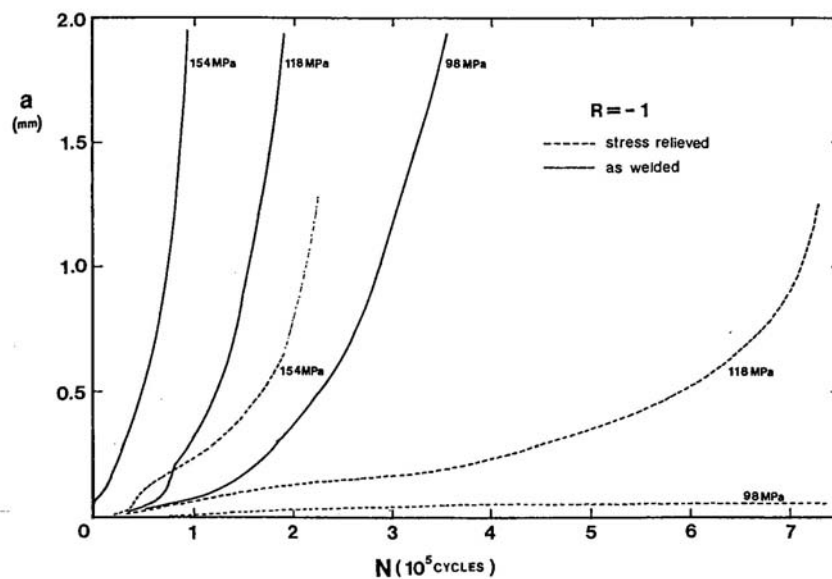


FIGURE 1. Measured growth of surface crack at weld toe for a cruciform fillet welded stiffened plate with alternating membrane load. (From [11].)

The case “stress relieved” represents a case with (almost no) residual stresses where a considerably lower crack growth rate is observed. The fact that the crack will be subject to tensile loads during a cycle can also be illustrated with the crack opening level. Figure 2 shows the evolution of the crack opening factor $U = (K_{\text{op}} - K_{\text{min}}) / (K_{\text{max}} - K_{\text{min}})$ plotted against crack length for the same load situation as in Fig. 1 based on strain gauge measurements along the weld toe on the membrane loaded plate. It is seen that the residual stress added to the applied stress will result in an almost fully open crack when the plate is subject to an alternating stress. For pulsating external stresses, $R = 0$, the effect of the residual stresses is smaller as the crack is already open, to a large extent already for the membrane load.

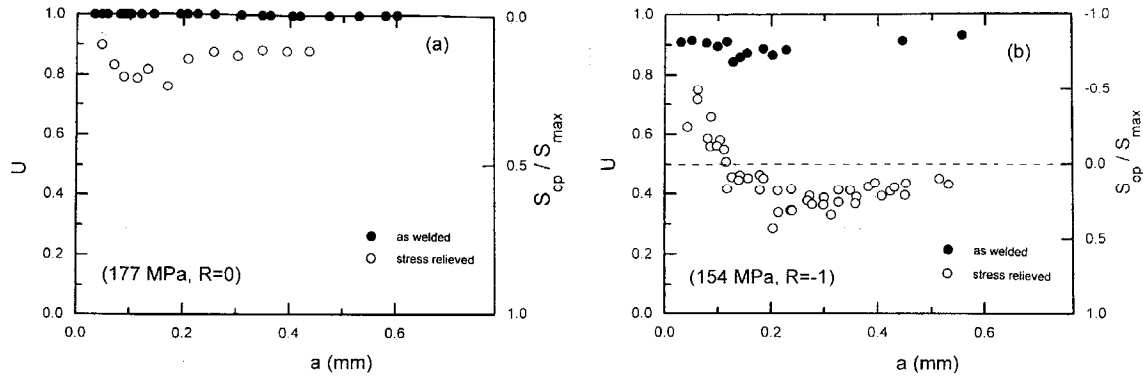


FIGURE 2. Measured influence of residual stress on the evolution of crack opening level with crack depth for surface cracks at weld toe of a fillet weld: $R = 0$ (left) and $R = -1$ (right). (From [12].)

When loading a welded joint containing a residual stress field with high tensile magnitudes there will be a redistribution of the residual stresses, a mechanical stress relaxation, and a reduction of the stress peaks. This effect will take place already during the first tensile cycles as can be demonstrated in experiments and in FE simulations, see for example [13-15]. As yielding most likely will occur, it is not possible to superpose the external stress field and the residual stress field. However, the relaxation of residual stress peaks may be estimated by assuming elastic shakedown (after the first stress cycle) using a cyclic stress strain curve [14]. Figure 3 shows the redistribution of the residual stress with distance from the toe of a fillet weld as measured by X-Ray technique [14].

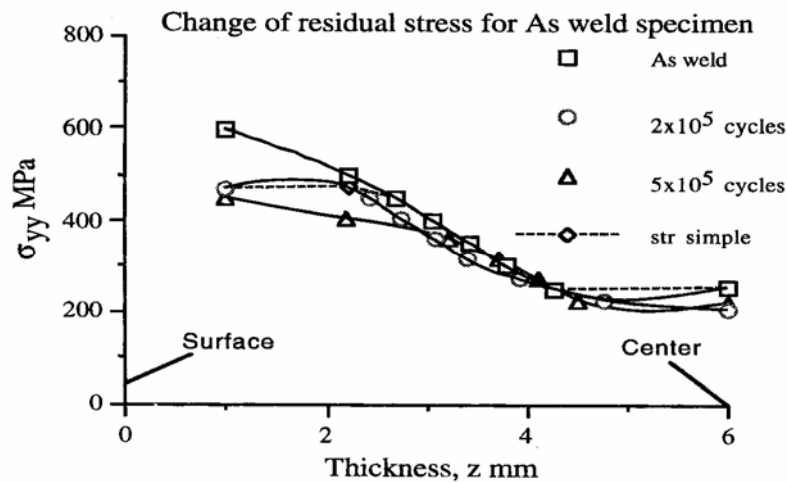


FIGURE 3. Measured stress redistribution near the weld toe in the thickness direction during cyclic loading of a stiffened plate with thickness 12 mm. (From [14].)

Three concepts of LEFM-based fatigue life estimates

Linear fracture mechanics based approaches for fatigue life estimates of crack propagation in a residual stress field have concerned many researchers during the past decades. The accuracy required in such analyses together with the computational effort available, have roused the demand for both analytical as well as finite element-based approaches for calculation of the crack driving force (i.e. stress-intensity factor or J -contour integral). In LEFM, the principle

of linear superposition is applicable where the K -factor contribution due to the residual stresses can contribute substantially towards satisfying the fracture criterion $K_I = K_{IC}$, where $K_I = K_I(\text{residual stress}) + K_I(\text{external loads})$. Special features of K -factors for residual stress fields are that they often vary along the border of the crack and also that they vary irregularly with crack size. This may have unforeseen effects on both fatigue and unstable crack propagation. In addition, the K -factor superposition technique has been employed by among others Wu and Carlsson [16], who performed calculations of welding residual stress-intensity factors for half-elliptical surface cracks in thin and thick plates. The FE method was used to calculate the stress-intensity factors from the residual stress field and the external loads, respectively. Wallentin et al. [17] used the same technique in the analysis of crack growth around railway wheel flats exposed to rolling contact loads, considering residual stresses due to formation of martensite under the wheel flats. An influence function method, based on Betti's reciprocity theorem, was applied to calculate the stress-intensity factors near the crack-tip in the wheel rim. In the SINTAP defect assessment procedure, [9], the superposition of stress-intensity factors as shown above is employed; however possible stress redistribution (reduction of residual stress peaks) is accounted for using a correction factor for K_I (residual stress). This effect is pronounced when assessing ductile static fracture with large plastic deformations.

The methodology described in the previous paragraph is suitable if the residual stress field can be accurately described by an analytical function or distribution, i.e. there is no need to estimate the residual stress field by numerical simulation. This is, however, of course not always the case since the residual stresses that occur during manufacturing or surface treatment processes can vary substantially through depth, and hence, they are preferably more accurately determined by FE simulation of the process itself. Another reason is also what type of fatigue assessment that is aimed for. Teng et al. [15], for example, present thermal elasto-plastic FE calculations of a butt weld. The calculated residual stress field is used in a phenomenological multi-axial fatigue theory model to estimate the fatigue life to crack initiation. Results using different strain based approaches for fatigue crack initiation were compared with experimental results for butt welded plates subject to membrane loads. Janosch et al. [18] used a local approach for fatigue crack initiation, the Dang Van criterion, to estimate the effect of residual stresses on the risk for fatigue in a fillet weld in a membrane loaded stiffened plate. Good agreement with experimental results was achieved by adding the initial residual stresses to the hydrostatic pressure caused by the external loads. Verreman and Nie [11] and Verreman et al. [19] performed analyses of short crack fatigue propagation in fillet welds, where the residual stress fields were calculated using a homogeneous (uncracked) FE model, and thereafter used in a fracture mechanics relation that accounts also for crack closure. Additionally, fracture assessment using an FE model containing a crack is often performed in a sequence, see Michaleris et al. [20]. Firstly, the residual stress and the corresponding displacement fields are calculated using a (homogeneous) FE model without a crack. Secondly, the residual stresses are interpolated to an FE model with the same geometry but now with the crack present in the model. The FE model with the crack is used for fracture mechanics analysis including residual stresses, for the current crack length, to calculate the stress-intensity factors or the J -contour integral. For LEM analysis of different crack lengths, it is common to have numerous FE models with different crack lengths. Strip-yield models are considered hybrid finite-element and continuum-mechanic models, and these models form the basis for several fatigue life prediction codes, see Newman [21]. FASTRAN is a fatigue life prediction code based on Elber's plasticity-induced crack closure concept and the effective stress-intensity factor range, see Newman [22]. The effective stress-intensity range is defined as the part of the applied stress range for which the crack front is fully open. The Dugdale model is used but modified to leave plastically deformed material in the wake

of the crack-tip; the plastic zone and the contact stress behind the crack-tip are obtained by superposition of two elastic problems. The effect of the welding residual stress field on uncertainties in fatigue life predictions was modelled by Josefson et al. [23], by including a third term according to Wang [24] in the superposition corresponding to the crack surface displacement caused by the welding residual stress field. The influence from the residual stress field is quantified by a mean stress S_m , added to the external load cycle S , as $S_m = H_{\text{weld}} / f_s$. Here, H_{weld} is defined by $K_{\text{weld}}(a) = \int_0^a \sigma_{\text{weld}}(x) m(x, a) dx = H_{\text{weld}} \sqrt{\pi a}$ and f_s is the geometry factor for the external load. The weight function $m(x, a)$ can be obtained numerically from Wu and Carlsson [25]. Note that the additional mean stress S_m depends on the crack length a , which means that the external stress S is updated continuously in the crack growth calculations in FASTRAN.

Hou and Lawrence [26] have also investigated the influence of crack closure in weldments using a strip-yield model which employs Newman's method of simulating crack closure. The influence of the weld-toe plastic deformation on crack closure was estimated using FE analysis and it was superposed linearly to the theory of the Dugdale-type crack: the total plastic stretches (TPS) = the notch plastic stretches from FE analysis (NPS) + the crack-tip plastic stretches from the theory of Dugdale-type crack (CTPS). The calculated TPS are used in the strip-yield model to estimate the crack-closure behaviour of a fatigue crack emanating from a notch root. Additionally, the strip-yield model calculates crack closure based on crack-face displacements when the external load is maximum and minimum. Instead of the basic concept for considering the effects of residual stresses in a strip-yield model, i.e. superposition of stress-intensity factors, Hou and Lawrence [26] used the crack-face displacements in the superposition for calculation of the CTPS. Hence, the magnitude of the CTPS in the range from a to $a + \rho_c$ (a is the crack length and ρ_c is the crack-tip plastic zone) can be obtained by superposing three elastic crack-face displacements: $\text{CTPS}(x) = u_{S_{\text{max}}}(x) + u_{\text{res}}(x) + u_o(x)$ where the first, second and third terms represent the elastic crack-face displacement caused by the maximum remote stress, the residual stress and the strip-yield load, respectively. The residual stress term is considered as described in Wang [24].

Design codes for welded joints

Fatigue design rules for welded constructions have been developed over a time period of some 40 years and they are now well established. Most fatigue design is based on the nominal stress method using a set of standard S - N curves, with the elastic nominal stress range $\sigma_r = \sigma_{\text{max}} - \sigma_{\text{min}}$ as stress measure, for different weld geometries, so called Detail Classes (FAT). Hence, the elastically determined nominal stress ranges at the weld joint, $\Delta\sigma$, shall be less than the fatigue resistance possibly corrected by a safety factor. The fatigue resistance for a welded joint is determined from full scale tests on welds (at constant amplitude), giving each weld geometry a certain fatigue class FAT. The fatigue class FAT includes the weld geometry, that is the fatigue notch factor K_f and the effect of the welding residual stress field. It is defined as the applied stress range $\Delta\sigma$ that for a given welded joint gives a fatigue life of $2 \cdot 10^6$ cycles (for a given risk for failure). The slope using logarithmic axes is normally taken as $-1/3$. In some countries, the design codes also distinguish the quality for the welded joint. For variable amplitude loading, a Palmgren-Miner linear damage accumulation rule is used, thus neglecting load sequence effects. Maddox and Razmjoo [27] review design methods for multi-axial loads. In these methods one normally assumes that S - N curves obtained under uni-axial loading are applicable when used in combination with an equivalent stress, like the von Mises effective stress or the maximum principal stress. For

variable amplitude loading, the Palmgren-Miner rule may be applied for each nominal stress components, normal and shear, using the appropriate $S-N$ design curves.

As an alternative to the nominal stress approach, the structural stress or hot spot stress approach has been proposed. This method considers the macro stress concentration and excludes the local stress concentration at a weld toe. A finite element, mesh size independent, based stress computation would thereby be possible. Fricke [28] gives an overview of the development of different approaches used in the fatigue design codes [29] including numerical fatigue analysis of welded joints. Maddox [30] reviews the current status of the design rules and presents results in certain areas where the codes may be improved; the effect of residual stresses, the scale effect, the treatment of multi-axial loads, the treatment of cumulative damage during variable amplitude loading and the possible presence of a fatigue limit.

Numerical examples on fatigue life and crack growth predictions

Simulation of rail welding and fatigue crack growth in rail welds

The two main rail welding procedures in use are flash butt welding and aluminothermic welding. Flash butt welding is performed mainly at welding plants, while aluminothermic welding is used for in-track welding. In both type of welds, lack-of-fusion defects are susceptible locations for crack growth, where the residual stresses caused by the rail welding process have considerable effect on crack growth behaviour. Skyttebol et al. [31] have investigated the effect of welding residual stresses on fatigue crack growth in rail welds. The study includes different sizes and locations of the cracks as well as different loading conditions. The simulations performed incorporate several steps, and calculations, to make the fatigue assessment of the weld as realistic as possible, see Fig. 4. The finite element (FE) method, using the commercial FE code ABAQUS/Standard [32], was used to simulate the welding process, the dynamic train-track response and the elasto-plastic stress response in the rail. The fatigue crack growth and propagation analyses were made in the commercial code SACC [33].

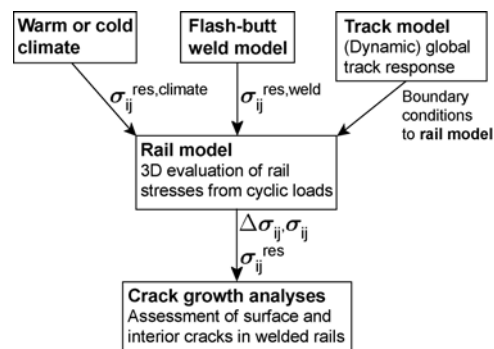


FIGURE 4. Flowchart of the fatigue evaluation of flash-butt welded rails. (From [31].)

The FE code ABAQUS/Standard was utilized for the finite element analysis of the flash-butt welding process. The weld simulation was performed in a sequence, starting with an electro-thermal analysis that provides a temperature field history to the subsequent thermo-mechanical analysis. The calculated residual stresses are found to be in good agreement with experimentally determined residual stresses in a welded rail, see Fig. 5 where x is the transverse direction of the rail, y is the vertical direction of the rail, and z is in the longitudinal direction of the rail.

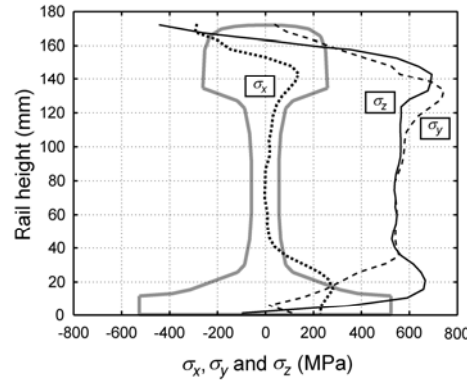


FIGURE 5. Residual stresses from flash-butt weld FE analysis in the centre of the weld. (From [31].)

The redistribution of residual stresses in the welded rail was simulated for a straight track, during heavy-haul operation conditions, using a train-track model called the FE tool, see Ringsberg et al. [34]. Three different axle loads were investigated, and for each axle load, four initial stress-state conditions of a rail were analysed with the FE tool:

- (a) residual stress-free rail,
- (b) residual stress field from the flash-butt welding process, $T_{\text{ref}} = 20^{\circ}\text{C}$,
- (c) residual stress field from the flash-butt welding process + superposed residual stresses from cold climate during the winter, $T_{\text{cold}} = -40^{\circ}\text{C}$, and
- (d) residual stress field from the flash-butt welding process + superposed residual stresses from a warm climate during the summer, $T_{\text{hot}} = 40^{\circ}\text{C}$.

It was found from the FE calculations that, apart from the contact zone at the rail head, the weld material experienced elastic shakedown after very few load passages. With the weld material subject to elastic conditions, linear elastic fracture mechanics can be used to study growth of the defects in the weld region. The code SACC [33] was employed for this purpose, using the calculated stress ranges from the FE tool. In addition, three different defects were considered: an embedded circular crack at mid level of the rail head subject to vertical stress ranges, an embedded circular crack in the rail head just above the web also subject to vertical stress ranges, and a half-circular surface crack at the lower part of the rail head subject to longitudinal stress ranges, see Skyttebol [31] for details. The first two cases correspond to inclusion defects or lack-of-fusion defects, while the third case corresponds to a crack starting from a defect caused by the final trimming of the web and rail head. The size of the crack area, A_{crack} , was varied between 5 and 100 mm². It was observed that the weld was more sensitive to surface cracks (growing in the rail longitudinal direction) than embedded cracks, in particular at the upper part of the web and lower rail head region where the stress ranges were large; $R = \sigma_{\text{min}} / \sigma_{\text{max}}$ was $R = 0.7 - 0.9$.

Mutton and Alvarez [35] studied the failure modes in aluminothermic rail welds under high axle load conditions; similar axle loads were investigated by Skyttebol et al. [31]. An extensive research program was undertaken to examine the long-term viability of aluminothermic welding procedures under heavy-haul conditions. The two main failures of the rail were vertical fractures and horizontal split-web fractures starting in the web in the centre of the weld. The latter failure mode was the dominating one which is also a greater derailment risk than vertical failures. Experimental results from Mutton et al. [35] show that

the stress range in the web may be higher for a weld in a curved track due to the torsion of the web. Depending on possible horizontal misalignment of the rail weld additional stress ranges may also appear in the weld region. Hence, the situation studied by Skyttebol et al. [31], a weld in a straight track, may not represent a severe loading case in terms of fatigue crack propagation. However, it gives a qualitative picture of fatigue growth of different defects in a rail weld.

Mechanical modelling of resistance spot welding

Spot welding of two (or three) sheets involves simultaneous heating and cooling and contact, achieved by clamping copper electrodes to the sheets. An accurate model would then include the interaction of electrical, thermal and mechanical fields as well as the microstructure evolution. Henrysson et al. [36] modelled spot welding of a single overlap specimen using the commercial FE code SYSWELD. High stress gradients were observed both in the FE analysis and in parallel experiments. This residual stress field was then transferred to a fully 3D FE model representing an overlap specimen. Fatigue loading was simulated by a cyclic loading of the specimen. The FE mesh used for the overlap specimen is shown in Fig. 6. The largest radial stress amplitude due to mechanical loading is normally found to appear at the perimeter of the nuggett. This was found also in [36], however, as the yield stress of the nuggett is about twice as high as in the base metal due to phase changes during welding, it was found that for higher membrane loads (with magnitudes normally found in car body structures) the material yields in each load cycle in the base metal (with the largest experienced plastic strains) leading to yielding during each load cycle, whereas the material is elastic at the nuggett perimeter during the cyclic loading. Figure 7 shows the calculated stress-strain curves for a overlap specimen (plate thickness 1 mm) subject to a pulsating external stress ($R = 0.1$) at two locations (A) at the nuggett perimeter and (B) in the base metal in one sheet. For reasonably high external loads the welding stresses are relaxed already after a few load cycles. Car body structures, or components of the car body, contain many spots. In mechanical analyses they are normally modelled using beam elements, thus considering their contribution to the stiffness but normally neglecting effects of welding residual stresses. Mean stress effects in fatigue life prediction can be explained by crack closure effects. This has been shown both by experiments and in FE simulations of growth of a crack from the nuggett perimeter [37].

Fatigue crack growth analysis of a butt welded plate

In several manufacturing operations a compressive stress is introduced at the surface of a structure to reduce growth of cracks initiated at the surface, case hardening [38], shot peening and different cold working processes to introduce compressive hoop stresses at the bore of a hole [39]. Stress coining is one such method by use of a transverse compression. The generation of residual stresses and the subsequent redistribution during operation were studied numerically and experimentally by Ogeman [40]. Figure 8 shows the plate geometry and the built-up and relaxation of coining stresses at the corner of the hole when the plate is subjected to the coining pressure followed by loading by an alternating membrane stress, $R = -1$, with continuously increasing amplitude. One finds that there will be a considerable redistribution when the operational load is applied.

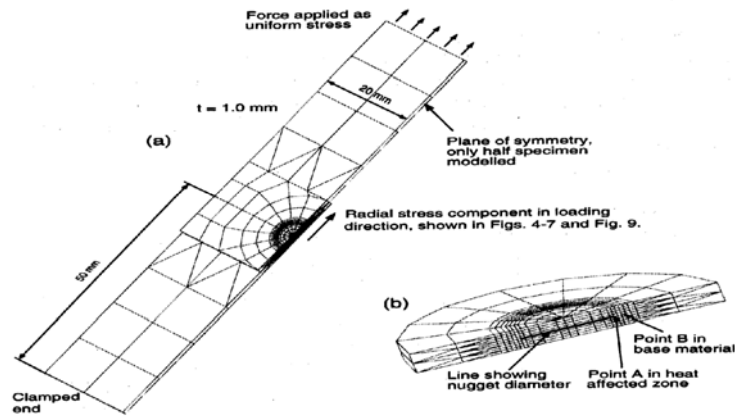


FIGURE 6. 3D FE mesh of an overlap specimen used in simulation of mechanical loading. Points included in fatigue analysis are shown. (From [36].)

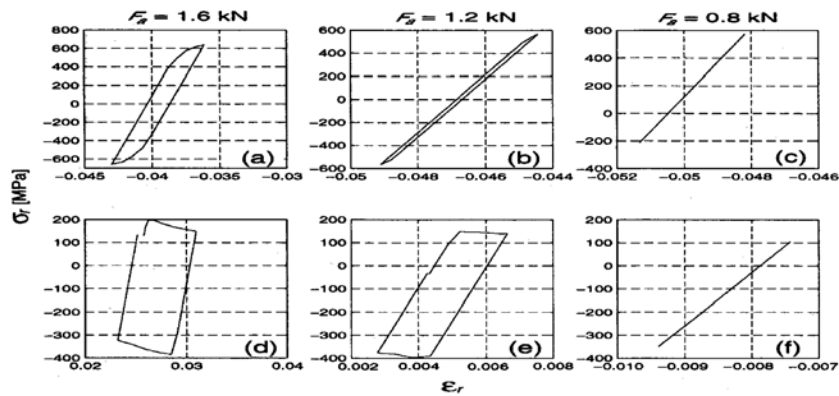


FIGURE 7. Results from calculated stress-strain curves for the third load cycle for an overlap specimen with a 5 mm nugget diameter exposed to different force amplitudes at $R = 0.1$: a), b) and c) point (A) in HAZ d), e) and f) point (B) in base material. (From [36].)

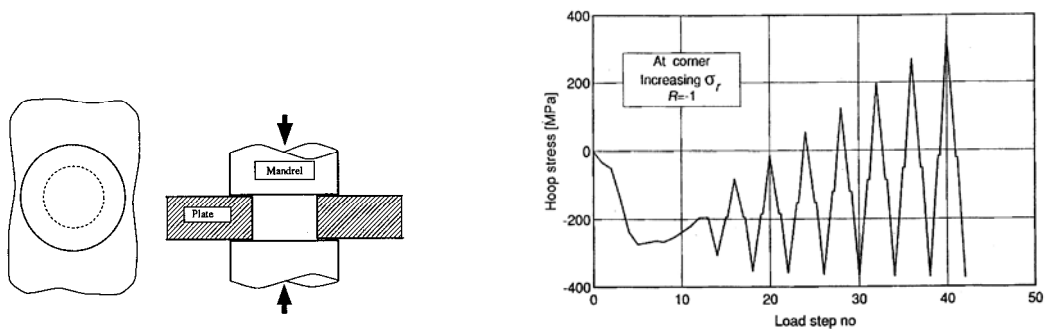


FIGURE 8. Left: Geometry of plate with hole, from [40]. Right: Calculated hoop stress redistribution at corner of hole during coining and subsequent membrane plate loading with $R = -1$ (From [41].)

To quantify the beneficial effect of stress coining on the growth of fatigue cracks, the fatigue life for quarter elliptic corner cracks and half-elliptic central cracks at bore of the hole was calculated integrating Paris law for crack growth, with modification for near threshold growth, and superposing the stress-intensity factors for the membrane hoop stress and the coining hoop stress [41]. Figure 9 shows the calculated fatigue life for a corner crack, defined as the number of cycles needed to propagate a crack to roughly half the plate thickness. In particular for $R = -1$, coining is seen to strongly reduce the fatigue life.

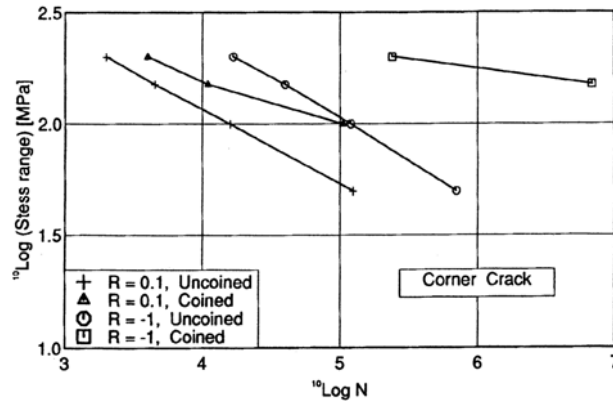


FIGURE 9. Calculated fatigue life for a corner crack subject to a membrane stress (From [41].)

Fatigue crack growth analysis of a butt welded plate

As mentioned above, one often finds experimentally that cracks of lengths 0.1 - 0.5 mm are created at weld toes already during the manufacturing process. The fatigue life may therefore be estimated using empirically-based relations for crack propagation, although for smaller crack lengths the cracks may be considered as “short”.

In Josefson et al. [23] the commonly used Paris law for stationary crack growth at constant amplitude was used for analysis of crack growth in a butt welded plate. Load ratio effects were introduced to account for plasticity-induced crack closure as proposed by Elber. The membrane loaded plate is shown in Fig. 10 where the plate width was $W = 90$ mm and the plate thickness was $h = 20$ mm. The plate was considered to be manufactured by butt welding and a hole, with the diameter $d = 26.6$ mm, drilled at the plate (and weld) centre line. The longitudinal welding residual stress was assumed to have the shape (after the hole was introduced) $\sigma_{\text{weld}}(x) = \sigma_0(e^{-px} - q)/(1 - q)$, where p and q are constants determined by the position of the zero level for σ_{weld} and the condition that $\int_0^{w/2} \sigma_{\text{weld}}(x)dx = 0$. A through-the-thickness crack was assumed to grow from the centre hole with current crack length a . The growth of the crack was calculated using Paris law employing the effective stress-intensity factor ΔK_{eff} for plasticity-induced crack closure, see Josefson et al. [23] for details. The crack opening stress was assumed to model load ratio effects as caused by plasticity-induced crack closure. It was obtained using the analytical crack closure model by Newman [42] and the crack growth program FASTRAN [22]. The effect of the welding residual stress field was modelled employing the approach by Wang [24], see previous section and Josefson et al. [23] for details.

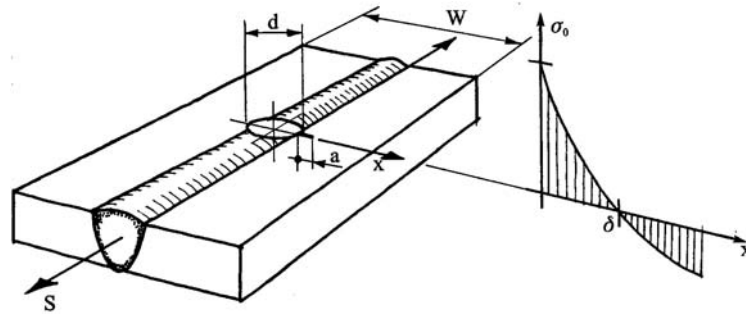


FIGURE 10. Geometry of the welded plate and shape of the welding residual stress field. (From [23].)

Figure 11 shows the calculated life N in (Mcycles) for some combinations of the two parameters controlling the shape of the welding residual stress field, σ_0 and δ for the external load ratio $R = -1$. In the calculations, the initial crack length was $a_0 = 0.2$ mm, the yield stress of the material taken as 350 MPa, and the parameters in the Paris law were $C = 3.9 \cdot 10^{-12}$ and $m = 3$ (stresses in MPa and crack lengths in m). The applied stress range was 140 MPa and the calculations were stopped when the crack length was roughly half the distance between the hole edge and the plate edge. Note that values for σ_0 were low, thus justifying a direct superposition, without stress relaxation, of external and residual stress-intensity factors.

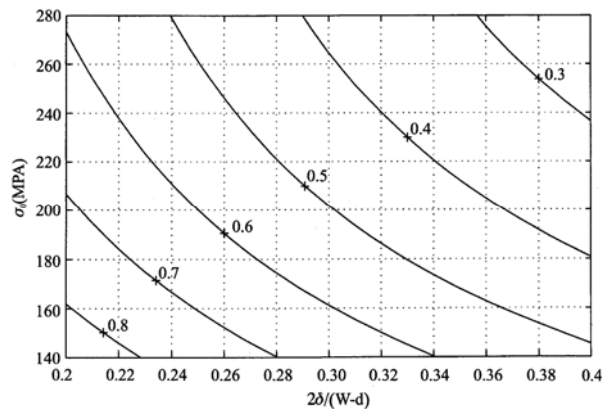


FIGURE 11. Calculated fatigue life (in Mcycles) for some different shapes of the welding residual stress field and $R = -1$ for the external load. (From [23]).

The results from the FASTRAN calculations were used in a statistical analysis where the uncertainty in calculated fatigue life was made based on the uncertainties in material data, weld geometry and weld process parameters. It was found that the variation in material parameters and the initial crack length were more important than the variation in the residual stress field.

Discussion

This presentation has focussed on the influence of manufacturing processes (where an initial defect is created) on the stress based fatigue behaviour. Hence the fatigue life consists only of a crack propagation phase. The crack growth is then controlled by the resulting stress

$\sigma_{\max} - \sigma_{\min}$ and the crack opening level U , thus defining the effective stress-intensity factor range ΔK_I .

To obtain the correct stress range and mean stress level acting at the critical point in the weld, the redistribution of the residual stresses during, possibly the first, cycles of the operational load must be considered. This means that, in principle, one can not superpose the external stress field and the initial stress field, or superpose the corresponding stress-intensity factors. Yet, almost all fracture mechanics based crack growth analyses employ this superposition, possibly because the stress redistribution during the first cycle may be computationally difficult as it has to be carried out using an elasto-plastic FE analysis. The technically interesting case of variable amplitude demands, in principle, that one follows the variation of stress range and crack closure for the load history. To acquire a better understanding of, in particular, load sequence effects, one would like to follow the crack development during the load history. This calls for the possibility of using adaptive FE techniques for simulation of continuous crack growth in an FE mesh. In such analyses, the orientation of crack growth as well as the redistribution of residual stresses during crack growth is incorporated.

The conservative assumption of residual stresses in welds reaching yield level is often questioned. Clearly, there exist several welding situations where this situation is not true [2], but also the mechanical stress relation that takes place will reduce the stress peaks. One could therefore anticipate that there may be an R -dependence for the fatigue life. Finally, below are three issues related to variable amplitude loading that are discussed in relation to design code development.

- How to incorporate load sequence effects. Several experimental investigations of welded structures show that there may be strong load sequence effects not accounted for using a linear damage accumulation (Palmgren-Miner) approach [30].
- Experiments on welds with load histories containing, for example, few cycles with stress ranges above the constant amplitude fatigue limit and many cycles below the fatigue limit, show that the stress ranges below the fatigue limit may be damaging. Thus, there seems to be no fatigue limit.
- The treatment of multi-axial loading cases. Current approaches in the design codes may not cover cases with complex loading, like when the principal stress directions change during the fatigue load cycle. One example is when the applied shear stress contribution is dominating and may give shear fatigue failure (Mode III) [30]. This is the case for torsion applied to tube or plate joints. Bäckström and Marquis [43] present experimental results for constant amplitude bending or tension and torsion experiments. From the different approaches, a modified critical plane model was found to give the best agreement with experiments.

References

1. Brust, F.W., In *Fatigue & Fracture Mechanics: 33rd Volume, ASTM STP 1417*, edited by R.S. Piascik and W.G. Reuter, ASTM International, West Conshohocken, PA, USA, 2001, 385–406.
2. Radaj, D., *Welding Residual Stresses and Distortion*, DVS-Verlag, Düsseldorf, Germany, 2003.
3. Lindgren, L.-E., *J. Therm. Stresses*, vol. **24**, 141–192, 2001.

4. Lindgren, L.-E., *J. Therm. Stresses*, vol. **24**, 195–231, 2001.
5. Lindgren, L.-E., *J. Therm. Stresses*, vol. **24**, 305–334, 2001.
6. Runesson, K., Skyttebol, A. and Lindgren, L.-E., In *Comprehensive Structural Integrity, Volume 3 Numerical and Computational Methods*, edited by R. de Borst and H.A. Mang, Elsevier, Oxford, UK, 2003, 255–320.
7. Dong, P., In *Proceedings of The Sixth International Conference on Residual Stresses - ICRS-6*, The Institute of Materials (IOM), London, UK, 2000, 1223–1238.
8. Dong, P., *Welding in the World*, vol. **46**, 24–31, 2002.
9. Stacey, A., Barthelemy, J.-Y., Leggatt, R.H. and Ainsworth, R.A., *Engng Fract. Mech.*, vol. **67**, 573–611, 2000.
10. Miller, K., In *Proceedings of the Seventh International Fatigue Congress - Fatigue '99*, edited by X.-R. Wu and Z.-G. Wang, Higher Education Press, Beijing, PRC, 1999, 15–39.
11. Nie, B., Verreman, Y. and Audoin, M., In *Proceedings of the International Conference on residual Stresses - ICRS2*, edited by G. Beck, S. Denis and A. Simon, Elsevier, London, UK, 1989, 965–970.
12. Verreman, Y. and Nie, B., *Fatigue Fract Engng Mater. Struct.*, vol. **19**, 669–681, 1996.
13. Takanashi, M. and Kamata, K., *Relaxation Behavior of Welding Residual Stresses by Fatigue Loading in Smooth Longitudinal Butt Welded Joints*, IIW Document XIII-1789-99, International Institute of Welding, 1999.
14. Lopez-Martinez, L., Lin Peng, R., Blom A.F. and Wang, D., In *Fatigue Design and Reliability*, edited by G. Marquis and J. Solin, ESIS Publication 23, Elsevier Science, Kidlington, Oxford, UK, 1999, 117–134.
15. Teng, T.-L., Fung, C.-P. and Chang, P.-H., *Engng Fail. Anal.*, vol. **10**, 131–151, 2003.
16. Wu, X.R. and Carlsson, J., *Engng Fract. Mech.*, vol. **19**, 407–426, 1984.
17. Wallentin, M., Bjarnehed, H.L. and Lundén, R., In *Proceedings of the Sixth International Conference on Contact Mechanics and Wear of Rail/Wheel Systems – CM2003*, edited by A. Ekberg, E. Kabo and J.W. Ringsberg, Vasastadens Bokbinderi AB, Sweden, 2003, 385–396.
18. Janosch, J.J., Debiez, S., Clerge, M. and Dang Van, K., In *IIW 50th Annual Assembly Conference: International Conference on Performance of Dynamically Loaded Welded Structures*, edited by S.J. Maddox and M. Prager, Welding Research Council, Inc., NY, USA, 1997, 265–272.
19. Verreman, Y. and Nie, B., In *IIW 50th Annual Assembly Conference: International Conference on Performance of Dynamically Loaded Welded Structures*, edited by S.J. Maddox and M. Prager, Welding Research Council, Inc., NY, USA, 1997, 240–253.
20. Michaleris, P., Kirk, M., Mohr, W. and McGaughy, T., In *Fatigue & Fracture Mechanics: 28th Volume, ASTM STP1321*, edited by J.H. Underwood, B.D. MacDonald and M.R. Mitchell, ASTM International, West Conshohocken, PA, USA, 1997, 499–514.
21. Newman, Jr J.C., In *Proceedings of the Eighth International Fatigue Congress – Fatigue 2002*, edited by A.F. Blom, Engineering Materials and Advisory Services Ltd. (EMAS), West Midlands, UK, 2002, 55–70.

22. Newman, Jr J.C., *FASTRAN-II – a fatigue crack growth structural analysis program*, NASA Langley Research Center, USA, NASA Technical Memorandum 104159, 1992.
23. Josefson, B.L., De Maré, J., Svensson, T. and Björklund, S., In *Engineering Against Fatigue*, edited by J.H. Beynon, M.W. Brown, R.A. Smith, T.C. Lindley and B. Tomkins, A.A. Balkema, Rotterdam, The Netherlands, 1999, 365–371.
24. Wang, G.S., *Engng Fract. Mech.*, vol. **46**, 909–930, 1993.
25. Wu, X.R. and Carlsson, J., *Weight Functions and Stress Intensity Factor Calculations*, Pergamon, Oxford, UK, 1991.
26. Hou, C.Y. and Lawrence, F.V., *Fatigue Fract. Engng Mater. Struct.*, vol. **19**, 683–693, 1996.
27. Maddox, S. and Razmjoo, G.R., *Fatigue Fract. Engng Mater. Struct.*, vol. **24**, 329–337, 2001.
28. Fricke, W., *Marine Struct.*, vol. **16**, 185–200, 2003.
29. Hobbacher, A., *Fatigue Design of Welded Joints and Components*, Abington Publishing, Cambridge, UK, 1996.
30. Maddox, S.W., *Welding in the World*, vol. **47**, 7–42, 2003.
31. Skyttebol, A., Josefson, B.L. and Ringsberg, J.W., Fatigue crack growth in a welded rail under the influence of residual stresses, Department of Applied Mechanics, Chalmers University of Technology, Göteborg, Sweden, Research Report 2003:6, 2003. (Accepted for publication in *Engng Fract. Mech.*)
32. Hibbitt, Karlsson and Sorensen Inc. *ABAQUS/User's Manual, version 6.4*, Pawtucket, RI, USA, 1998.
33. SACC Version 4.1, revision 9, Det norske Veritas, Stockholm, Sweden, 2003.
34. Ringsberg, J.W., Bjarnehed, H., Johansson, A. and Josefson, B.L., *Proc IMechE, Part F, J. Rail Rapid Transit*, vol. **214**, 7–19, 2000.
35. Mutton, P.J. and Alvarez, E.F., *Engng Fail. Anal.*, vol. **11**, 151–166, 2004.
36. Henrysson, H.-F., Abdulwahab, F. Josefson, B.L. and Fermér, M., *Welding in the World*, vol. **43**, 55–63, 1999.
37. Henrysson, H.-F., *Fatigue Fract. Engng Mater. Struct.*, vol. **25**, 1175–1185, 2002.
38. Limodin, N., Verreman, Y. and Tarfa, T.N., *Fatigue Fract. Engng Mater. Struct.*, vol. **26**, 811–820, 2003.
39. Ofsthun, M., *Int. J. Fatigue*, vol. **25**, 1223–1228, 2003.
40. Ogeman, R.T., *Int. J. Mech. Sci.*, vol. **36**, 1121–1132, 1994.
41. Josefson, B.L., Karlsson, S. and Ogeman, R., *Engng Fract. Mech.*, vol. **47**, 13–27, 1994.
42. Newman, J.C., In *Methods and Models for Predicting Fatigue Crack Growth under Random Loading, ASTM STP 748*, edited by J.B. Chang and C.M. Hudson, ASTM International, West Conshohocken, PA, USA, 1981, 53–84.
43. Bäckström, M. and Marquis, G., *Fatigue Fract. Engng Mater. Struct.*, vol. **24**, 279–291, 2001.